Journal Pre-proof

Interspecies complementation identifies a pathway to assemble SNAREs

Leonardo A. Parra-Rivas, Mark T. Palfreyman, Thien N. Vu, Erik M. Jorgensen

Interspecies complementation identifies a pathway to assemble SNAREs

Leonardo A. Parra-Rivas*[1], Mark T. Palfreyman*[1], Thien N. Vu*[1], and Erik M. Jorgensen[1,2]

1 Howard Hughes Medical Institute, School of Biological Sciences, University of Utah, Salt

Lake City, Utah, 84112-0840

2 Lead contact: Erik M. Jorgensen, Howard Hughes Medical Institute, Department of Biology,

257 South 1400 East, University of Utah, Salt Lake City, Utah, 84112-0840, Phone: 801-585-

3517, Fax: 801-581-2174, jorgensen@biology.utah.edu

*These authors contributed equally to this work.

Abstract

Unc18 and SNARE proteins form the core of the membrane fusion complex at synapses. To understand the functional interactions within the core machinery we adopted an 'interspecies complementation' approach in *C. elegans*. Substitutions of individual SNAREs and Unc18 proteins with those from yeast fails to rescue fusion. However, synaptic transmission could be restored in worm-yeast chimeras when two key interfaces were present: an Habc-Unc18 contact site and an Unc18-SNARE motif contact site. A constitutively open form of Unc18 bypasses the requirement for the Habc-Unc18 interface. These data suggest that the Habc domain of syntaxin is required for Unc18 to adopt an open conformation; open Unc18 then templates SNARE complex formation. Finally, we demonstrate that the SNARE and Unc18 machinery in the nematode *C. elegans* can be replaced by yeast proteins and still carry out synaptic transmission, pointing to the deep evolutionary conservation of these two interfaces.

Introduction

In all eukaryotic cells, the fusion of transport vesicles to target membranes requires SNARE and SM (Sec1/Munc18) proteins (Rothman, 2014; Südhof, 2014). For each membrane target, a distinct set of SNARE and SM proteins is used. Fusion at the plasma membrane is mediated by as specific subset of these proteins: In the case of synapses, the SNARE protein on the vesicle is synaptobrevin, the SNAREs on the plasma membrane are syntaxin and SNAP25, and the SM protein is Unc18. The SNARE domains interact at their N-termini and zipper into a four-helix bundle that drives membrane fusion (Gao et al., 2012; Hanson et al., 1997; Min et al., 2013; Pobbati et al., 2006; Sørensen et al., 2006; Sutton et al., 1998; Xu et al., 1999; Zorman et al., 2014).

Syntaxin is composed of 5 domains: an N-terminal peptide, a three-helix bundle called the Habc domain, a linker domain, a SNARE domain, and a transmembrane domain (Fig. S1A). To facilitate trafficking, the synaptic SM protein Unc18 (UNC-18/ Munc18) binds syntaxin in the closed conformation with the Habc domain folded over the SNARE motif (Arunachalam et al., 2008; Han et al., 2009; Hata et al., 1993; Medine et al., 2007; Misura et al., 2000; Rickman et al., 2007; Rowe et al., 2001). At the synapse, SNARE assembly requires syntaxin to be in the open conformation. This transition is thought to be mediated by Unc13

proteins (UNC-13/Munc13) (Gong et al., 2021; Hammarlund et al., 2007; Ma et al., 2011; Magdziarek et al., 2020; Richmond et al., 2001; Yang et al., 2015). Unc18 is required at the final stages to chaperone the SNAREs through their assembly (André et al., 2020; Baker et al., 2015; Gong et al., 2021; Jiao et al., 2018; Lai et al., 2017; Rodkey et al., 2008; Shu et al., 2020; Sitarska et al., 2017). The activation steps between open syntaxin and SNARE complex formation are not fully understood.

To understand the role of the domains of syntaxin in vesicle fusion, we adopted an 'interspecies complementation' strategy in the nematode *C. elegans*. Instead of studying mutations generated in syntaxin by random mutagenesis, we substituted entire domains with homologous regions from syntaxins of distant species. In most cases, domain substitutions severely disrupted syntaxin function. The expression of interacting UNC-18 orthologs from the cognate species were then used to restore function. Chimeric versions of UNC-18 further refined interfaces between binding targets.

Notably, replacing the worm Habc domain of syntaxin with the yeast Habc domain severely disrupted neurotransmission. Further replacement of UNC-18 with the yeast homolog Sec1 improved function minimally. Synaptic function was only restored when a chimeric Sec1 could simultaneously interact with both the Habc domain and the SNARE domains. The physiological phenotypes were mirrored by defects in synaptic vesicle docking, demonstrating that morphological docking is a manifestation of SNARE pairing (Imig et al., 2014). Finally, an 'open' form of worm Unc18 protein (UNC-18) could partially bypass the requirement for its interaction with its cognate Habc.

Together, the genetic data suggest a model in which UNC-13 signals the presence of a tethered synaptic vesicle and 'opens' syntaxin. In the 'open' form the Habc domain of syntaxin no longer occludes the SNARE domain. The Habc domain is further required for the transition of UNC-18 from an inactive closed state to an active 'open' configuration. UNC-18 in the open conformation binds the SNARE domains of synaptobrevin and syntaxin to template SNARE assembly.

Surprisingly, we also found that substituting the entire yeast SNARE complex along with Sec1 also provided significant rescue – the synapse still functions with yeast proteins, underscoring the conserved functions of these proteins in very different molecular contexts and cellular environments.

3

Results

Syntaxin Habc domain is required for neurotransmission

As a first step toward understanding the function of the domains of syntaxin, we engineered chimeric molecules with the yeast homolog Sso1p. We swapped the N-peptide, the Habc domain, the linker domain, and the SNARE motif (Fig. S1A), and assayed rescue as single-copy transgenes in the null mutant of syntaxin. In *C. elegans,* syntaxin null animals (referred to using the alternative name, *syx-1,* rather than *unc-64,* for clarity) are lethal (Saifee et al., 1998). To study syntaxin null mutants, we rescued animals to adulthood by expressing syntaxin in acetylcholine and glutamate head neurons (Hammarlund et al., 2007). This mosaic approach was used in all instances where the syntaxin transgene did not rescue lethality.

The functions of the chimeric proteins were determined by locomotion assays (Fig. 1A,B) and sensitivity to the acetylcholine–esterase inhibitor aldicarb (Fig. 1C) – resistance to the drug implies a reduced level of acetylcholine release (Mahoney et al., 2006). The N-peptide swap only exhibited subtle changes to locomotion, consistent with some previous experiments (Meijer et al., 2012; Park et al., 2016; Vardar et al., 2021), but not all (Hu et al., 2007; Shen et al., 2007, 2010; Zhou et al., 2013). The replacement of the linker domain resulted in significant defects in locomotion and aldicarb sensitivity. The replacement of the SNARE motif with the yeast Sso1p sequence eliminated syntaxin function in both locomotion and aldicarb sensitivity assays. This is not surprising, given its role in the formation of the SNARE complex. The SNARE motif swap also exhibited reduced syntaxin in axons (Fig. S2A), which is expected since the closed conformation is required for trafficking and the closed conformation requires extensive interactions between the SNARE motif and the Habc domain (Arunachalam et al., 2008; Fan et al., 2007; Han et al., 2009; McEwen and Kaplan, 2008; Medine et al., 2007; Rickman et al., 2007; Rowe et al., 1999, 2001).

The most intriguing result was that the replacement of the syntaxin Habc domain with the yeast Sso1p Habc domain (yeast-Habc chimera) reduced aldicarb sensitivity and resulted in as severe a defect in locomotion as the SNARE motif swap. The yeast-Habc chimera behaves identically to a full deletion of the Habc domain (Rathore et al., 2010) and to the syntaxin null animals (Fig. 1B-C), demonstrating the importance of this domain. The Habc domain is a conserved, autonomously folding, three-helix bundle (Fernandez et al.,

4

1998), which occludes the SNARE domain, thus preventing the interaction with other SNARE proteins (Dulubova et al., 1999; Misura et al., 2000). This architecture suggests an inhibitory function for the Habc domain. In agreement, the deletion of the Habc domain from Sso1 increases SNARE complex assembly over 2000-fold (Nicholson et al., 1998). However, the deletion of the yeast Vam3 Habc domain (Lürick et al., 2015), the mouse syntaxin Habc domain (Vardar et al., 2021; Zhou et al., 2013), and the worm syntaxin Habc domain (Rathore et al., 2010) all decreased fusion. The decrease in fusion could be attributed to poor trafficking (Fan et al., 2007; Medine et al., 2007; Yang et al., 2006) or poor expression (Vardar et al., 2021; Zhou et al., 2013). We observed some reduced trafficking of syntaxin to axons in our yeast-Habc chimera (Fig. S2A). Again, the Habc-SNARE mismatch should cause syntaxin to adopt the open state. Consistent with this expectation, a constitutively open form of syntaxin (Dulubova et al., 1999) exhibited a similar trafficking defect as the Habc-SNARE mismatch present in the yeast-SNARE chimera and the yeast-Habc chimera (Fig. S2A). However, 70% of syntaxin was properly trafficked and localized to axons in the yeast-Habc chimera.

To determine at what point in evolution the Habc domain acquired characteristics to support synaptic transmission, we swapped in the Habc domains from placozoa, choanoflagellates, and yeast (sequence identities 46%, 38%, and 23% respectively; Fig. S1B). The placozoan, *Trichoplax adhaerens*, is a basal multicellular metazoan that possesses the molecular machinery for synapses but lacks neurons and synapses at an anatomical and ultrastructural level (Smith et al., 2014). The choanoflagellate, *Monosiga brevicollis*, is a flagellated eukaryote, which can assume single-celled or colonial forms, and represent a stage prior to the advent of multicellularity (Brunet and King, 2017). By definition, the communication in choanoflagellates takes place between organisms rather than between cells within an organism. The yeast, *Saccharomyces cerevisiae*, is a single-celled organism that communicates to neighbors by the exocytosis of diffusible pheromones (Merlini et al., 2013).

Defects in neurotransmission in nematodes expressing syntaxin Habc chimeras were ascertained by locomotion (Fig. 2A,B), aldicarb sensitivity (Fig. 2C), and electrophysiology (Fig. 2D,E). Trafficking was assayed by fluorescence microscopy (Fig. S2B). All of the syntaxin Habc chimeras were tagged with GFP at the N-terminus. Tagging syntaxin at the N-terminus resulted in a mild reduction in miniature postsynaptic currents (minis/s: wild type:

48.5 ± 7.0; GFP-tagged syntaxin: 33.0 ± 2.7). Surprisingly, both the placozoan and the choanoflagellate chimeras provided a substantial rescue despite a sizable sequence divergence (Fig. S1B). In *Trichoplax*, the rescue was indistinguishable from worm syntaxin (minis/s: worm: 33.0 ± 2.7; *Tricho* Habc chimera: 29.9 ± 3.3). The choanoflagellate chimera provided an intermediate rescue (minis/s: choano Habc chimera: 12.9 ± 2.0). Only the yeast chimera was unable to provide any rescue and was indistinguishable from animals with a full deletion of the Habc domains (Rathore et al., 2010) and from syntaxin null animals (minis/s: *syx-1* null: 0.03 ± 0.02; yeast-Habc chimera: 0.10 ± 0.06). These results argue that the function of the Habc domain must predate synaptic transmission and, to a large extent, even metazoans.

Habc-Unc18 interactions required for SNARE assembly

The Habc domain in the closed conformation of syntaxin is known to bind Unc18 proteins (Misura et al., 2000). The yeast Unc18 and syntaxin orthologs, Sec1p and Sso1p, bind one another and function in yeast exocytosis (Aalto et al., 1993; Carr et al., 1999; Novick and Schekman, 1979). We reasoned that matching the yeast Habc domain with the cognate Sec1p protein might provide rescue by restoring an interaction interface between these two proteins. In the presence of the yeast-Habc chimera, expression of Sec1p provided a small, but significant, improvement of locomotory function and miniature postsynaptic currents (Fig. 3A,B,C, minis/s: yeast-Habc chimera + Sec1p: 0.13 ± 0.02; yeast-Habc chimera + UNC-18: 0.02 ± 0.00). Similarly, pairing the choanoflagellate Habc chimera with the choanoflagellate SM protein provided significant rescue for locomotion and neurotransmitter release (Fig. S3A,B).

Unc18 and syntaxin have both been reported to play a role in synaptic vesicle docking (Hammarlund et al., 2007; Toonen et al., 2006; Voets et al., 2001; Weimer et al., 2003; de Wit et al., 2006). We assayed docked vesicles by reconstructing synaptic regions from serial electron micrographs. The yeast-Habc chimera exhibited 91% and 95% reduction in docking at acetylcholine and GABA synapses, respectively (Fig. 3D,E, docked vesicles: ACh, wild type: 3.9 ± 2.2; yeast-Habc chimera: 0.35 ± 0.14; Fig. S4B,C, docked vesicles: GABA, wild type: 13 ± 3.5; yeast-Habc chimera: 0.7 ± 0.5), similar to *syx-1 unc-18* double mutants (Fig. 3D,E) and *syx-1* null animals (Hammarlund et al., 2007). Consistent with the electrophysiological recordings, docking was not restored by matching the yeast-Habc chimera with the yeast

6

conspecific Sec1p (Fig. 3D,E, docked vesicles: ACh, yeast-Habc chimera + Sec1p: 1.9 ± 1.2; Fig. S4B,C, docked vesicles: GABA, yeast-Habc chimera + Sec1p: 1.4 ± 0.9). Importantly, the docking defects were not a result of decreased synaptic vesicle numbers (Fig. S4A). We conclude that the binding of Unc18 and the Habc domain is not sufficient to restore synaptic functions: other interactions must be required.

The SM family proteins, which include Unc18, are known to interact with SNARE domains, potentially to template SNARE pairing (Jiao et al., 2018; Lee et al., 2020; Ma et al., 2015; Wang et al., 2019). The crystal structure of the yeast SM protein Vps33 with its cognate SNAREs indicates that the Qa-SNARE and the R-SNARE are bound in what may be a half-zippered SNARE complex (Baker et al., 2015). This structure is likely to have captured an SM protein in the middle of templating the SNAREs. The lack of templating of the synaptic SNAREs by Sec1p could explain the lack of rescue in our Habc-SM match. To test this model, we restored templating to our chimeric proteins. Although yeast Vps33 is only 16% identical to either yeast Sec1p or worm UNC-18, structure predictions and sequence alignments generated by the SWISS-MODEL and Clustal Omega Webservers, respectively (Higgins and Sharp, 1988; Schwede et al., 2003) identified potential residues in worm UNC-18 that would interact with SNARE domains (Fig. S5). We narrowed the list of residues to those that were not conserved between the yeast Sec1p and the worm UNC-18. We replaced these potential SNARE interacting residues on the yeast Sec1p with the corresponding worm residues to generate a 'Sec1p chimera' (Fig. S5). Co-expressing the yeast-Habc chimera with the Sec1p chimera yielded a dramatic rescue of synaptic transmission (Fig. 4A,B,C, minis/s yeast-Habc chimera: 0.10 ± 0.06; yeast-Habc chimera + Sec1p chimera: 9.62 ± 1.64). Locomotion and mini rates were improved 60-fold compared to the strain matching only the yeast Habc domain with yeast Sec1p. Thus, when the Unc18 protein is able to interact conspecifically with both the Habc and SNARE motifs, synaptic function is restored (in this case the yeast Habc domain with yeast Sec1p, and the worm UNC-18 SNARE-interacting residues with worm SNARE motifs).

The dramatic rescue observed with the Sec1p chimera was not due to gain-of-function activity. In the presence of the worm Habc domain, the Sec1p chimera did not confer rescue and was no different than an *unc-18* null mutant (Fig. S6). Note that the *C. elegans* genome encodes a paralog of *unc-18*, T07A9.10, which is expressed ubiquitously, and likely explains the unusually high level of synaptic transmission in *unc-18* null mutants

7

compared to equivalent deletions in other organisms (Cao et al., 2017; Taylor et al., 2021). Thus, the absence of rescue of *unc-18* null mutants, indicates that the Sec1p chimera can only function when it can interact with both the Habc domain and the SNARE motifs.

Docking was also restored when the Sec1p chimera could interact with both the Habc domain and the SNARE motifs (Fig. 4D,E ACh docked vesicles, wild type: 3.9 ± 2.2 ; yeast-Habc chimera + Sec1p chimera: 3.8 ± 1.9). Interestingly, although the rescue of docking is complete, the rescue of vesicle fusions is only partial (29%) (minis/sec: WT, 33.0 ± 2.7; yeast-Habc chimera + Sec1p chimera, 9.6 ± 1.6) (Fig. 4A-E and Fig. S4B).

In the experiments described so far, the SNARE domains were from the worm. To determine if yeast SNARE motifs can drive fusion at worm synapses, we expressed yeast Sec1p with the entire yeast SNARE complex including the yeast Habc domain (Fig. S7- S8). Remarkably, the yeast Sec1p and the yeast SNARE complex provided substantial rescue – the range was similar to animals co-expressing the yeast-Habc chimera and the Sec1p chimera (Fig. 4A,B,C, minis/s, yeast SNARE complex: 6.70 ± 2.10; yeast-Habc chimera + Sec1p chimera: 9.62 ± 1.64). Importantly, this rescue was completely lost when the Habc domain of yeast syntaxin (Sso1p) was replaced by the Habc domain from worm syntaxin (Fig. 4A,B,C minis/s yeast SNARE complex: 6.70 ± 2.10; yeast SNARE complex with worm Habc: 0.09 ± 0.03). Similarly, docking was rescued by the yeast Sec1p-SNARE complex, but not if the Habc domain was replaced by the worm Habc domain (Fig. 4D,E, ACh wild type: 3.9 ± 2.2; yeast SNARE complex with yeast Habc: 6.9 ± 1.9; yeast SNARE complex with worm Habc: 1.9±1.2). In fact, docking was increased almost 2-fold with yeast machinery compared to the wild type, suggesting that some docked vesicles are fusion-compromised in this strain. Fusion-incompetent vesicles could arise due to inefficient coupling of vesicles to calcium channels via UNC-13, poor pairing with the calcium-sensing machinery, synaptotagmin and complexin, or possibly misassembled SNAREs. It is also possible the yeast machinery is not interacting with the machinery that restricts docking to the active zone of neurons, resulting in ectopically docked vesicles in this strain.

Thus, the Habc domain of syntaxin must interact with UNC-18, and UNC-18 must interact with the SNARE domains to nucleate conspecific SNARE pairing. These experiments further suggest that templating SNARE assembly is a deeply conserved feature in SM proteins: this SNARE-binding interface is functionally conserved from SM proteins used in yeast lysosome fusion to synaptic Unc18 proteins in organisms with nervous systems.

Syntaxin Habc domain is required to open Unc18

Unc18 proteins can adopt two conformations in crystal structures: a 'closed' conformation (Misura et al., 2000) or an 'open' conformation (Hu et al., 2011). Specifically, the Unc18 domain 3a transitions from a compact furled loop (closed state) to an extended helical structure (open state) (Hu et al., 2011). A P335A mutation in Unc18 favors the helical extension and increases rates of synaptic vesicle fusion (Han et al., 2014; Munch et al., 2016; Parisotto et al., 2014; Park et al., 2017).

One possible model is that the Habc domain is required to convert UNC-18 into the open state. If true, then the constitutively open form of UNC-18 should bypass the requirement for the Habc interaction to UNC-18. Animals expressing the yeast-Habc chimera are indistinguishable from syntaxin null animals, but expression of the constitutively open form of UNC-18 increased speed 6-fold (Fig. 5A; μm/s yeast-Habc chimera + wild-type UNC-18: 0.43 ± 0.32; yeast-Habc chimera + open-UNC-18: 2.83 ± 1.68). Although the rescue was not complete, open-UNC-18 increased neurotransmitter release as assayed by aldicarb-sensitivity (Fig. 5B) and by electrophysiology (Fig. 5C,D; minis/s yeast-Habc chimera: 0.10 ± 0.06; yeast-Habc chimera + open UNC-18: 1.80 ± 0.70). We also found that open-UNC-18 could bypass the defects seen in the choanoflagellate-Habc chimera (Fig. S3C,D). These data suggest that open state of UNC-18 acts downstream of the Habc interaction with UNC-18.

To determine if 'open' UNC-18 bypassed the requirement for the Habc domain in docking, we performed electron microscopy on the strain expressing open-UNC-18 with the yeast Habc-chimera. The 'open' form of UNC-18 bypasses the requirement for the UNC-18-Habc interaction in docking (Fig. 5E,F). Unlike locomotion and physiology, the rescue of docking is complete.

Together, these data suggest a model in which the Habc domain is required to transform UNC-18 from the closed state to the open state, which allows UNC-18 to bind to the SNARE domains and nucleate the SNARE complex formation (Fig. 6).

Discussion

To identify evolutionarily conserved protein interactions in synaptic vesicle fusion, we used an 'interspecies complementation' approach to determine the function of the Habc domain in the nematode *C. elegans*. To be most effective, interspecies complementation starts from 'zero output', that is, the replacement of a single component from another

9

species resembles a null mutation. We found the worm syntaxin Habc domain could be functionally replaced with those from the Placozoan *Trichoplax* or the Choanoflagellate *Monosiga.* Thus, the conservation of *physical* interactions between the Habc domain and the synaptic machinery predated the evolution of synapses and, indeed, the evolution of metazoans. Eventually, we had to rely on the highly divergent SNARE machinery in yeast to obtain 'zero output'. The yeast-Habc chimera resembles the syntaxin null mutant and a full deletion of the Habc domain (Rathore et al., 2010).

Fusion was restored by a complex in which two interfaces were species matched: first, the Habc domain and the SM protein, and second the SM protein 'grooves' and the SNARE motifs. However, an Habc to UNC-18 mismatch could be bypassed if the UNC-18 protein was locked in the open conformation, thereby suggesting that the Habc domain might function to convert UNC-18 from a closed to open conformation to template SNAREs. Both of these genetic configurations rescued docking, but did not fully rescue fusion rates. One possible reason for incomplete rescue of fusion is that the yeast-Habc syntaxin chimera fails to dock synaptic vesicles adjacent to calcium channels. Unc13 is required for vesicle docking (Hammarlund et al., 2007). In addition, Unc13 couples docked vesicles to calcium channels (Tan et al., 2022) because it binds both Habc domain of syntaxin (Betz et al., 1997) and interacts with calcium channels via RIM (Brockmann et al., 2020; Kaeser et al., 2011). Syntaxin in the open state bypasses the requirement for UNC-13 in vesicle docking, but fusion is only partially restored (Hammarlund et al., 2007). Because of the mismatch between the Habc domain and the SNARE motif, the yeast-Habc syntaxin chimera is predicted to be in the 'open' state and dock vesicles independent of Unc13. It is possible that these promiscuously docked vesicles are not coupled to calcium channels, and therefore are not fusion competent. Alternatively, vesicles may be docked near calcium channels but the SNAREs may be misassembled (Lai et al., 2017). Likewise, 'open' UNC-18 may bypass crucial steps needed in localizing the fusion machinery near calcium channels or in proofreading SNARE assembly, leading to docked but fusion compromised vesicles.

Two recent structures suggest that the core function of SM proteins is to template SNARE assembly. First, we used the structure of the yeast lysosomal SM protein, Vps33, to map residues in Sec1 that could potentially be modified to interact with worm SNAREs (Baker et al., 2015). Vps33 only has very weak homology with UNC-18, and yet the engineered Sec1 provided significant rescue. The rescue we observed provides the strongest

evidence yet for the physiological importance of the templating functions of the SM proteins, which thus far have only been minimally explored in vivo (André et al., 2020). Second, the recent structure of the yeast Golgi SNARE Tlg2 bound to Vps45 indicates that SM proteins can interact with the Habc domain and the SNARE domain in an open conformation (Eisemann et al., 2020). Although similar structural data are not available for Sec1 or Unc18 proteins, binding experiments indicate Unc18 is able to interact with open syntaxin (Christie et al., 2012; Colbert et al., 2013; Rickman et al., 2007; Shen et al., 2007). Finally, our interspecies complementation underscores the universal nature of the interactions between SM proteins and SNAREs that nucleate SNARE assembly.

Taken together our findings suggest a model for the regulatory interactions leading to the SNARE pairing at the synapse (Fig. 6). The active zone protein UNC-13 is thought to convert syntaxin from a closed to an open state (Hammarlund et al., 2007; Ma et al., 2011; Magdziarek et al., 2020; Richmond et al., 2001; Yang et al., 2015), although this role has been disputed (McEwen et al., 2006; Tien et al., 2020). Templating is a late step and requires the open conformation of UNC-18. We therefore speculate that in the open state, the Habc domain of syntaxin converts UNC-18 to an open conformation. Based on the crystal structure of Vps33, the open form of UNC-18 binds the SNARE domains of synaptobrevin and syntaxin to nucleate SNARE assembly (Baker et al., 2015; Sitarska et al., 2017). SNAP-25 is thought to be the last SNARE to enter the complex (Jiao et al., 2018; Kalyana Sundaram et al., 2021; Wang et al., 2019), although the order is still in dispute (Lee et al., 2020).

Perhaps the most remarkable result is that the core fusion machinery from yeast can function in neurotransmission. We do not yet understand how or indeed whether the yeast SNAREs and SM protein are able to couple with the specialized calcium-sensing machinery used in synaptic vesicle fusion. However, the rescue confirms that the functional interactions provided by the SNAREs and their partner SM proteins have remained largely constant from yeast to man, even within very different molecular contexts and cellular environments.

Limitation of the study

Our study identifies two interfaces between syntaxin and Unc18 that are required for their functional interactions. Chimeric yeast-worm proteins provide functional rescue at the *C. elegans* neuromuscular junction only when these interfaces are species matched. The interface between the syntaxin Habc domain and UNC-18 can be partially bypassed by an

open form of UNC-18. The identification of these interfaces and the bypass by UNC-18 relies solely on genetic studies, and conclusions would be strengthened by biophysical or structural studies. For instance, data demonstrating that Habc binding directly promotes the open state of UNC-18. However, the results are consistent with published structural studies of yeast SNARE homologs bound to SM proteins.

Acknowledgements

Figure Legends

Fig. 1. Syntaxin domains differentially contribute to neurotransmission.

A, (Top) Cartoons depicting syntaxin domains and the chimeras generated by swapping in the corresponding domains from yeast Ssop1. All the chimeras and the rescuing wild-type control ('worm SYX-1') are GFP-tagged and integrated into the syntaxin null background, *syx-1.* (Bottom) Representative locomotion trajectories collected for 1 min. **B,** Average locomotion rates (speed) of 20 animals are compared for the same four strains. Data are displayed as scatter dot plots with mean and SEM. Each point represents an animal. **C,** Average paralysis time courses after aldicarb exposure (n=3 independent experiments on 20 worms per experiment). Error bars represent SEM. n.s. > 0.05; *** < 0.001 (Student's two-tailed t-test).

Fig. 2. The syntaxin Habc is required for neurotransmission.

A, (top) Cartoons depicting syntaxin with the Habc domain swapped in from the placozoan *Trichoplax adhaerens*; the choanoflagellate *Monosiga brevicollis*; and yeast *Saccharomyces*

cerevisiae. All the chimeras and the wild-type control (worm SYX-1) are GFP-tagged and expressed in the *syx-1* null strain. The GFP tag mildly decreases function compared to the true wild-type (WT) control. (bottom) Representative locomotion trajectories collected for 1 min. **B,** Average locomotion speed of 20 animals compared for the same four strains. **C,** Average paralysis time courses after aldicarb exposure (n=3 independent experiments on 20 worms per experiment). **D,** Representative traces of endogenous miniature postsynaptic currents (minis) recorded from the body muscle of syntaxin chimeras. **E,** Quantification of the mini frequency. Neuronal expression of GFP tagged worm syntaxin rescued mini frequency of syntaxin null animals, but not to wild-type levels (WT, 48.5 ± 7.0 minis/second; n=6 vs. worm SYX-1, 33 ± 2.7 minis/second; n = 11 vs. *syx-1* null, 0.03 ± 0.019 minis/second; n = 6). Mini frequency in Trichoplax Habc chimeras (29.9 ± 3.2 minis/second; n = 9) was not different from rescued worm syntaxin. The average rate of fusion measured from choanoflagellate Habc chimeras (12.9 ± 1.9 minis/second; n = 12) and yeast-Habc chimeras (0.1 ±0.06 minis/second; n = 8) was significantly lower than that measured from the syntaxin rescued strain. Speed and mini frequency are displayed as scatter plots with mean and SEM. Each point represents a single animal. n.s. > 0.05; * < 0.05; *** < 0.001 (Student's two-tailed t-test). Error bars in aldicarb curves represent the SEM.

Fig. 3: Matching the Habc domain with Unc18 provides only minimal rescue

A, Average locomotion rates (speed) in, from left to right: syntaxin null animals; *syx-1 unc-18* double mutants; the yeast-Habc chimera; the yeast-Habc chimera overexpressing worm UNC-18; and the yeast-Habc chimera overexpressing Sec1p (yeast Unc18). **B,** Quantification of the mini frequency in the same five strains, all were similarly defective in synaptic transmission: *syx-1* null: 0.03 ± 0.019 minis/second, n = 6; *syx-1 unc-18* null: 0.08 ± 0.017 minis/second, n = 10; yeast-Habc chimera: 0.10 ± 0.057 minis/second, n = 8; yeast-Habc chimera overexpressing worm UNC-18: 0.02 ± 0.005 minis/second, n = 17; yeast-Habc chimera overexpressing Sec1p: 0.13 ± 0.021 minis/second, n = 22. Note, *syx-1* null and yeast-Habc are reproduced from Fig. 2. **C,** Representative traces of endogenous miniature postsynaptic currents (minis) recorded from the body muscle. **D,** Quantification of docked synaptic vesicles at acetylcholine synapses in the *syx-1 unc-18* double mutants, the yeast-Habc chimera, the yeast-Habc chimera overexpressing worm UNC-18, and the yeast-Habc chimera overexpressing Sec1p (yeast UNC-18). All had similarly reduced docking compared

to wild-type animals (docked SVs/ per ACh synapse: the wild type, 3.9±0.48, n=21; *syx-1 unc-18*, 0.95 ± 0.15 docked SV/synapse, n=20; yeast-Habc chimera, 0.35 ± 0.14, n=31; yeast-Habc chimera overexpressing UNC-18: 1.3 ± 0.21, n=19; yeast-Habc chimera overexpressing Sec1p: 1.9 ± 0.31, n=15). **E,** Representative electron micrographs of the neuromuscular junctions in the ventral nerve cord in the respective strains. Arrows indicate docked vesicles. All micrographs are displayed at the same magnification. Scale bar represents 100nm. Grouped data are displayed as scatter plots with mean and SEM. In locomotion assays and physiological assays each point represents one animal; in EM each point represents a synapse. n.s. > 0.05; *** < 0.001 (Student's two-tailed t-test for locomotion and physiological assays; Mann-Whitney for EM).

Fig. 4. Synaptic transmission is restored with two interaction interfaces: Unc18 – Habc and Unc18 – SNARE domain.

A, Average locomotion speed in, from left to right: the chimeric yeast-Habc chimera overexpressing Sec1p (yeast Unc18); the yeast-Habc chimera overexpressing the Sec1p chimera (yeast Unc18) with the SNARE interactions restored; syntaxin mutants overexpressing the full yeast SNARE complex and Sec1p without a matching Habc interaction; syntaxin mutants overexpressing the full yeast SNARE complex and Sec1p with a matching Habc interaction. **B,** Quantification of the mini frequency in the same four strains. When the two interaction surfaces are restored, synaptic transmission is rescued: yeast-Habc chimera overexpressing Sec1p: 0.13 ± 0.021 minis/second, n = 22; yeast-Habc chimera overexpressing the Sec1p chimera: 9.62 ± 1.636 minis/second, n = 12; overexpression of yeast SNARE complex with worm Habc + overexpression of Sec1p: 0.09 ± 0.033 minis/second, n = 11; overexpression of yeast Habc-SNARE with yeast Habc + overexpression of Sec1p: 6.70 ± 2.095 minis/second, n = 11). Note, yeast-Habc chimera + overexpression of Sec1p is reproduced from Fig. 3. **C,** Representative traces of endogenous miniature postsynaptic currents (Minis) recorded from the body wall muscle.

D, Quantification of docked synaptic vesicles in the yeast-Habc chimera overexpressing Sec1p; the yeast-Habc chimera overexpressing Sec1p with the SNARE interactions restored; syntaxin mutants overexpressing the full yeast SNARE complex and yeast Sec1p without a matching Habc interaction; syntaxin mutants overexpressing the full yeast SNARE complex and Sec1p with a matching Habc interaction; and wild-type animals. When the two

14

interaction surfaces are restored synaptic vesicle docking is restored (docked SVs/ per ACh synapse: yeast-Habc chimera + overexpression of Sec1p: 1.9 ± 0.31, n=15; yeast-Habc chimera + overexpression of the Sec1p chimera: 3.8 ± 0.47, n = 16; overexpression of the yeast SNARE complex with worm Habc + overexpression of Sec1p: 0.95 ± 0.093, n = 19; overexpression of the yeast SNARE complex with yeast Habc + overexpression of Sec1p: 6.9 ± 0.49, n = 15; wild type, 3.9±0.48, n=21). Note that the wild type, and the yeast-Habc chimera with overexpression of Sec1p, are the same data as Fig. 3d. **E,** Representative electron micrographs of the neuromuscular junctions in the ventral nerve cord in the respective strains. Arrows indicate docked vesicles. All micrographs are displayed at the same magnification. Scale bar represents 100nm. Grouped data are displayed as scatter plots with mean and SEM. In locomotion assays and physiological assays each point represents one animal; in EM each point represents a synapse. n.s. > 0.05; ** < 0.01; *** < 0.001 (Student's two-tailed t-test for locomotion and physiological assays; Mann-Whitney for EM).

Fig. 5. Syntaxin Habc domain opens Unc18.
A, Expression of P334A UNC-18 mutation 'Open UNC-18' in the yeast-Habc chimera background increased the locomotion speed 6-fold (n=20). **B,** Locked open UNC-18 makes yeast-Habc chimeras more sensitive to aldicarb than WT UNC-18 – indicating a restoration of ACh release in the open UNC-18 background. **C,** Open UNC-18 in yeast-Habc chimera increased the frequency of the endogenous miniature postsynaptic currents compare to yeast-Habc chimeras expressing WT UNC-18 (yeast-Habc chimera + overexpression of UNC-18: 0.02 ± 0.005 minis/second, n = 17; yeast-Habc chimera + overexpression of open-UNC-18: 1.80 ± 0.704 minis/second, n = 12). **D,** Representative traces of the endogenous miniature postsynaptic currents from indicated genotypes. **E,** Open UNC-18 restores docking to the yeast-Habc chimeras. Representative electron micrographs of the neuromuscular junctions in the ventral nerve cord in the animals expressing the yeast-Habc chimera with worm UNC-18 (left) or 'open' worm UNC-18 (right). All micrographs are displayed at the same magnification. Scale bar represents 100nm. **f,** Quantification of docking in the same two strains (yeast-Habc chimera + overexpression of UNC-18: 1.3 ± 0.21 docked SV/synapse, n=19; yeast-Habc chimera + overexpression of open UNC-18: 4.6 ± 0.36 docked SV/synapse, n=21). Note: yeast-Habc chimera + overexpression of UNC-18 data and sample micrograph are the same as Fig. 3d. Speed, mPSC frequency and docking are displayed as scatter plots

with mean and SEM. In locomotion assays and physiological assays each point represents one animal; in EM each point represents a synapse. n.s. > 0.05; ** < 0.01; *** < 0.001 (Student's two-tailed t-test for locomotion and physiological assays; Mann-Whitney for EM). Error bars in aldicarb sensitivity curves represent the SEM.

Fig. 6. Model of syntaxin Habc domain function.

In step 1, Unc18 binds closed syntaxin during trafficking to axons. In step 2, the active zone protein Unc13 converts syntaxin to the open configuration. In step 3, the Habc domain then converts Unc18 to an open conformation. In step 4, open Unc18 binds the SNARE domains of syntaxin and synaptobrevin, to align and nucleate SNARE complex assembly. In step 5, SNAP-25, complexin and synaptotagmin are recruited by unknown mechanisms to form a SNARE complex fully 'primed' for fusion. Our results do not explicitly exclude an alternative sequence of steps; for example, the 'opening' of UNC-18 could precede the 'opening' of syntaxin.

STAR Methods

RESOURCE AVAILABILITY

Lead contact

Requests for reagents, resources and information should be directed to Erik Jorgensen (**jorgensen@biology.utah.edu**).

Material availability

All *C. elegans* strains and plasmids generated in this study are available upon request from the lead contact.

Data and code availability

- All data reported in the paper will be shared by the lead contact upon request.

- This paper does not report any original code.

- Additional information needed to reanalyze the data in this paper is available from the lead contact.

EXPERIMENTAL MODEL AND SUBJECT DETAILS

All *Caenorhabditis elegans* strains used in this study were maintained on E. coli OP50- seeded NGM plates at 20°C (for experiments) or 15°C (for longer term storage). All experiments were conducted on adult hermaphrodites. A list of strains used in this paper can be found in the KEY RESOURCES TABLE below.

METHOD DETAILS

Strains

All strains were maintained on *E. coli* OP50- seeded NGM plates according to standard methods. Syntaxin null worms are paralyzed and arrest at the first larval stage (L1), which leads to lethality (Saifee et al., 1998). Some of the interspecies chimeras used in our study were unable to rescue *unc-64(js115)* syntaxin null phenotype (referred to using the

17

alternative name *syx-1* in text). To bypass the lethality, we used mosaic animals expressing wild-type syntaxin (Hammarlund et al., 2007) in the acetylcholine neurons of the head; this expression is sufficient to rescue syntaxin null mutants to adulthood. The null allele *unc-18(md299)* is a complete deletion of the locus; the strain is uncoordinated by viable (Weimer et al. 2003). For the *syx-1 unc-18* double mutant we expressed both syntaxin and UNC-18 in the acetylcholine head neurons. These mosaic animals were used in all cases where the syntaxin chimera was unable to rescue lethality (see Table T1 for a complete list of strains used in this work).

Molecular Biology

All plasmids were made using the Invitrogen multisite Gateway cloning technique. To build the rescuing construct for *unc-64(js115)* (syntaxin null animals), the neuronal UNC-64A cDNA was amplified from a worm cDNA library and cloned into Gateway entry vectors. This parental construct was used to engineer all syntaxin chimeras in this study. Domain replacement was performed by insertion of the corresponding synthetic gene fragments (Integrated DNA Technologies (IDT)) and assembled by Gibson cloning. The resulting [1-2] entry clones were recombined with a [4–1] entry vector containing the synaptotagmin promoter and a GFP tag (pEGB348); a [2–3] entry vector with the let-858 3'UTR; and the [4–3] destination vector (pCFJ201) using LR clonase (Invitrogen). Plasmids were inserted into the worm genome as a single copy using the MosSCI technique (Frøkjaer-Jensen et al., 2008) or expressed as extrachromosomal arrays for overexpression experiments. Similarly, UNC-18 rescuing constructs were obtained by cloning the UNC-18 cDNA or the synthetic Sec1p cDNA (from Biomatik) into the Gateway entry vectors. These plasmids were also used to generate the open UNC-18 mutant and the Sec1p chimera. In both cases, synthetic gene fragments with the desired nucleotide modification were cloned using Gibson assembly. The open UNC-18 mutant was obtained by mutation of the "hinge" proline (P334A) in UNC-18 domain 3a. To build the Sec1p chimera we introduced worm residues in the groove and cleft domains of Sec1p. To identify these substitutions we used the crystal structure of the yeast SM protein Vps33 with its cognate SNAREs (Baker et al., 2015). Residues from the Vps33 predicted to binds Nyv1 and Vam3 (PDB code 5BV0 and PDB code 5BUZ, respectively) were mapped into Sec1p based on secondary structure predictions generated by the SWISS-MODEL Webserver (Schwede et al., 2003) and sequence alignments obtained with Clustal

18

Omega (Higgins and Sharp, 1988) (S5). Using a pymol script we identified potential contact residues in Sec1p within 4 Angstrom that are not conserved between yeast and worm.

Imaging

Nematodes were immobilized using 25 mM sodium azide (NaN_3) and mounted on 3% agarose pads on glass slides. All images were acquired as Z-stacks using a Pascal LSM5 confocal microscope (Carl Zeiss) with a 63x 1.4NA oil objective. Ventral cord images were taken with the cord facing toward the objective. Fluorescent intensity was quantified using Image J software. Axon intensity was obtained by drawing a region of interest around the ventral nerve cord including the soma (total intensity) and subtracting the soma intensity. Data was analyzed using one-way ANOVA followed by Bonferroni's post-test and reported as mean ± SEM.

Worm tracking and speed analysis

To compare worm tracks, a single young adult worm was placed on a NGM plate seeded with OP50. After 1 minute, the animal was removed and a track picture was taken with a Stingray camera (Allied Vision Technologies model). Worm tracks were then drawn on a WACOM touchscreen monitor, x,y coordinates, and length measurements were determined using an ImageJ macro. ImageJ x,y coordinates were transformed into a scalable vector graphics file (svg) using a Matlab script developed in the Jorgensen lab. In Fig. S8, we allowed the animals to move for 5 minutes, instead of the customary 1 minute, to better distinguish between animals with severe locomotion defects.

To measure the speed, 20 animals for each strain were filmed for 2 minutes. Animals with severe locomotion defects were filmed for 30 minutes. Videos were generated using Wormtracker system (MBF Bioscience). Videos were then analyzed and average speed computed using WormLab software built in with the tracker system.

Aldicarb assays

Aldicarb sensitivity was assessed using 20 young adult worms on NMG plates containing 2 mM aldicarb. Worms were scored for paralysis at 10 minutes intervals for 6 hours. Worms were considered paralyzed when there was no movement in response to three taps to the head and tail with a platinum wire. Once paralyzed, worms were removed from the plate.

Each genotype was tested blind three times and paralysis curves were generated by averaging paralysis time courses for each plate.

Electrophysiology

Electrophysiological recordings were performed as follows (Richmond and Jorgensen, 1999; Richmond et al., 1999). Briefly, worms were immobilized with cyanoacrylate glue (Aesculap Histoacryl; BBraun Inc.) and a lateral incision was made to expose the ventral medial body muscles. The preparation was treated with collagenase (type IV; Sigma-Aldrich) for 15 seconds at a concentration of 0.5 mg/mL. The muscle was voltage-clamped using the whole-cell configuration at a holding potential of −60 mV. All recordings were performed at 21°C using an EPC-9 patch clamp amplifier (HEKA), which runs on an ITC-16 interface (HEKA). Data were acquired using Pulse software (HEKA). Data analysis and graph preparation were performed using Pulsefit (HEKA), Mini Analysis (Synaptosoft), and Igor Pro (Wavemetrics). Data are presented scatter plots, where each point represents one animal, with the mean ± standard error of the mean overlayed.

Electron microscopy

Electron microscopy experiments were performed as follows (Watanabe et al., 2013). Briefly, ten young adult worms were placed into a 100-um deep specimen carrier (type A and B) along with space-filling 5% bovine serum albumin in M9 buffer. Samples were frozen with a Leica EM-ICE high-pressure freezer. Freeze substitution was performed in a Leica EM AFS2 system. Frozen samples were fixed with 1% glutaraldehyde, 1% osmium tetroxide, and 1% water in anhydrous acetone for 24 hours at -90°C. The samples were warmed to -20°C at 5°C/hour, held at -20°C for 16 hours, and subsequently brought to room temperature (20°C, at 10°C/hour). Fixed animals were isolated from the specimen carrier and embedded in Epon-Araldite resin. Two random animals from each genotype were sectioned. ~250 ultrathin (33-40 nm) serial sections for each animal were collected on a Leica microtome (Ultracut UC7). The sections were post-stained with 2.5% uranyl acetate in 70% methanol for five minutes before imaging. Serial micrographs of the ventral nerve cords were collected in a transmission-mode scanning electron microscope (Zeiss GeminiSEM 300). ATLAS 5 was used to acquire images in a semi-automated fashion.

Synaptic morphometry was performed blind to genotype. Micrographs from serial sections encompassing a single synapse were collected as an image stack. A synapse was

20

defined as all profiles containing the presynaptic dense projection plus a flanking profile from each side of the dense projection (Watanabe et al., 2013). If more than two synaptic profiles were missing (section loss, occluding schmutz, etc.), the synaptic series was excluded from the analysis. The stacks of serial synaptic profiles were then randomized. Stacks were then segmented for features, such as total synaptic vesicle numbers, and docked vesicles. A synaptic vesicle was considered docked if the vesicle membrane touches the plasma membrane (0 nm) without lighter pixels between the vesicle and plasma membranes (Hammarlund et al., 2007). Acetylcholine and GABA synapses were segmented based on the *C. elegans* the reconstruction of the connectome from serial electron micrographs (White et al., 1986). Data are presented scatter plots, where each point represents one synapse, with the mean ± standard error of the mean overlayed.

Multiple Sequence Alignment Analysis and Model Interpretation

Protein sequences were retrieved from Uniprot via Jalview's sequence fetcher (Waterhouse et al., 2009) and aligned with the Clustal Omega Webserver with default parameters (Higgins and Sharp, 1988). For the syntaxin alignment shown in S1, mouse (uniprot O35526), worm (uniprot O16000-2), *Trichoplax* (uniprot B3S4L5), *Monosiga* (uniprot A9UTG5), and yeast (uniprot P32867) sequences were used. Alignment in S5 used the Vps33 sequence from *C. thermophilum* (uniprot G0SCM5) and UNC-18 sequences from mouse (uniprot A2ARS2), worm (wormbase UNC-18a 591aa, Note: the uniprot sequence P34815 673aa, is an anomalous sequence that appends 91 N-terminal amino acids from a region 5' of the *unc-18* gene), *Trichoplax* (uniprot B3RPC7), *Monosiga* (uniprot A9V0L3), and yeast (uniprot P30619). Alignment in S7 for synaptobrevin used sequences from worm (uniprot O02495) and yeast (uniprot P1109). Similarly, SNAP-25 alignment used sequences from worm (uniprot A5PEW5) and yeast (uniprot P40357).

All figures containing models (S1B and S5) were prepared with Chimera and ChimeraX (Pettersen et al., 2004, 2021).

QUANTIFICATION AND STATISTICAL ANALYSIS

Data in scatter plot graphs present single observations (points) and are shown as mean ± standard error of the mean (SEM). Data was analyzed for significance with a Student's two-tailed t-test for locomotion, physiology, and imaging. For electron microscopy we used a Mann-Whitney analysis. Further details are presented in the figure legends. All the tests

were performed using GraphPad Prism 8.3. A level of $P < 0.05$ was considered significant. In all grouped data analysis significance is represented as follows: ns > 0.05; * < 0.05; ** < 0.01; *** < 0.001.

Author Contributions

L.A.P. initiated the project with guidance from E.M.J. L.A.P., E.M.J., M.T.P., and T.N.V. designed the experiments. L.A.P. conducted all behavioral, aldicarb, and imaging experiments. M.T.P. conducted electrophysiological experiments. T.N.V. conducted EM experiments. L.A.P., M.T.P., and T.N.V. analyzed the data. L.A.P., E.M.J., M.T.P., and T.N.V. wrote the manuscript.

Declaration of interests

The authors declare no competing interests. L.A.P. is currently employed in the Department of Pathology, University of California, San Diego, 9500 Gilman Drive, La Jolla, CA, USA.

References

Aalto, M.K., Ronne, H., and Keränen, S. (1993). Yeast syntaxins Sso1p and Sso2p belong to a family of related membrane proteins that function in vesicular transport. EMBO J. *12*, 4095–4104.

André, T., Classen, J., Brenner, P., Betts, M.J., Dörr, B., Kreye, S., Zuidinga, B., Meijer, M., Russell, R.B., Verhage, M., et al. (2020). The Interaction of Munc18-1 Helix 11 and 12 with the Central Region of the VAMP2 SNARE Motif Is Essential for SNARE Templating and Synaptic Transmission. ENeuro *7*, ENEURO.0278-20.2020.

Arunachalam, L., Han, L., Tassew, N.G., He, Y., Wang, L., Xie, L., Fujita, Y., Kwan, E., Davletov, B., Monnier, P.P., et al. (2008). Munc18-1 is critical for plasma membrane localization of syntaxin1 but not of SNAP-25 in PC12 cells. Mol. Biol. Cell *19*, 722–734.

Baker, R.W., Jeffrey, P.D., Zick, M., Phillips, B.P., Wickner, W.T., and Hughson, F.M. (2015). A direct role for the Sec1/Munc18-family protein Vps33 as a template for SNARE assembly. Science *349*, 1111–1114.

Betz, A., Okamoto, M., Benseler, F., and Brose, N. (1997). Direct interaction of the rat unc-13 homologue munc13-1 with the N terminus of syntaxin. J. Biol. Chem. *272*, 2520–2526.

Brockmann, M.M., Zarebidaki, F., Camacho, M., Grauel, M.K., Trimbuch, T., Südhof, T.C., and Rosenmund, C. (2020). A Trio of Active Zone Proteins Comprised of RIM-BPs, RIMs, and Munc13s Governs Neurotransmitter Release. Cell Rep. *32*, 107960.

Brunet, T., and King, N. (2017). The Origin of Animal Multicellularity and Cell Differentiation. Dev. Cell *43*, 124–140.

Cao, J., Packer, J.S., Ramani, V., Cusanovich, D.A., Huynh, C., Daza, R., Qiu, X., Lee, C., Furlan, S.N., Steemers, F.J., et al. (2017). Comprehensive single-cell transcriptional profiling of a multicellular organism. Science *357*, 661–667.

Carr, C.M., Grote, E., Munson, M., Hughson, F.M., and Novick, P.J. (1999). Sec1p binds to SNARE complexes and concentrates at sites of secretion. J. Cell Biol. *146*, 333–344.

Christie, M.P., Whitten, A.E., King, G.J., Hu, S.-H., Jarrott, R.J., Chen, K.-E., Duff, A.P., Callow, P., Collins, B.M., James, D.E., et al. (2012). Low-resolution solution structures of Munc18:Syntaxin protein complexes indicate an open binding mode driven by the Syntaxin N-peptide. Proc. Natl. Acad. Sci. U. S. A. *109*, 9816–9821.

Colbert, K.N., Hattendorf, D.A., Weiss, T.M., Burkhardt, P., Fasshauer, D., and Weis, W.I. (2013). Syntaxin1a variants lacking an N-peptide or bearing the LE mutation bind to Munc18a in a closed conformation. Proc. Natl. Acad. Sci. U. S. A. *110*, 12637–12642.

Dulubova, I., Sugita, S., Hill, S., Hosaka, M., Fernandez, I., Südhof, T.C., and Rizo, J. (1999). A conformational switch in syntaxin during exocytosis: role of munc18. EMBO J. *18*, 4372–4382.

Eisemann, T.J., Allen, F., Lau, K., Shimamura, G.R., Jeffrey, P.D., and Hughson, F.M. (2020). The sec1/munc18 protein vps45 holds the qa-snare tlg2 in an open conformation. ELife *9*, 1–18.

Fan, J., Yang, X., Lu, J., Chen, L., and Xu, P. (2007). Role of H(abc) domain in membrane trafficking and targeting of syntaxin 1A. Biochem. Biophys. Res. Commun. *359*, 245–250.

Fernandez, I., Ubach, J., Dulubova, I., Zhang, X., Südhof, T.C., and Rizo, J. (1998). Three-dimensional structure of an evolutionarily conserved N-terminal domain of syntaxin 1A. Cell *94*, 841–849.

Frøkjaer-Jensen, C., Davis, M.W., Hopkins, C.E., Newman, B.J., Thummel, J.M., Olesen, S.-P., Grunnet, M., and Jorgensen, E.M. (2008). Single-copy insertion of transgenes in *Caenorhabditis elegans*. Nat. Genet. *40*, 1375–1383.

Gao, Y., Zorman, S., Gundersen, G., Xi, Z., Ma, L., Sirinakis, G., Rothman, J.E., and Zhang, Y. (2012). Single reconstituted neuronal SNARE complexes zipper in three distinct stages. Science *337*, 1340–1343.

Gong, J., Wang, X., Cui, C., Qin, Y., Jin, Z., Ma, C., and Yang, X. (2021). Exploring the Two Coupled Conformational Changes That Activate the Munc18-1/Syntaxin-1 Complex. Front. Mol. Neurosci. *14*, 785696–785696.

Hammarlund, M., Palfreyman, M.T., Watanabe, S., Olsen, S., and Jorgensen, E.M. (2007). Open syntaxin docks synaptic vesicles. PLoS Biol. *5*, 1695–1711.

Han, G.A., Park, S., Bin, N.R., Jung, C.H., Kim, B., Chandrasegaram, P., Matsuda, M., Riadi, I., Han, L., and Sugita, S. (2014). A pivotal role for pro-335 in balancing the dual functions of Munc18-1 domain-3a in regulated exocytosis. J. Biol. Chem. *289*, 33617–33628.

Han, L., Jiang, T., Han, G.A., Malintan, N.T., Xie, L., Wang, L., Tse, F.W., Gaisano, H.Y., Collins, B.M., Meunier, F.A., et al. (2009). Rescue of Munc18-1 and -2 double knockdown reveals the essential functions of interaction between Munc18 and closed syntaxin in PC12 cells. Mol. Biol. Cell *20*, 4962–4975.

Hanson, P.I., Roth, R., Morisaki, H., Jahn, R., and Heuser, J.E. (1997). Structure and conformational changes in NSF and its membrane receptor complexes visualized by quick-freeze/deep-etch electron microscopy. Cell *90*, 523–535.

Hata, Y., Slaughter, C.A., and Südhof, T.C. (1993). Synaptic vesicle fusion complex contains unc-18 homologue bound to syntaxin. Nature *366*, 347–351.

Higgins, D.G., and Sharp, P.M. (1988). CLUSTAL: a package for performing multiple sequence alignment on a microcomputer. Gene *73*, 237–244.

Hu, S.-H., Latham, C.F., Gee, C.L., James, D.E., and Martin, J.L. (2007). Structure of the Munc18c/Syntaxin4 N-peptide complex defines universal features of the N-peptide binding mode of Sec1/Munc18 proteins. Proc. Natl. Acad. Sci. *104*, 8773.

Hu, S.H., Christie, M.P., Saez, N.J., Latham, C.F., Jarrott, R., Lua, L.H.L., Collins, B.M., and Martin, J.L. (2011). Possible roles for Munc18-1 domain 3a and Syntaxin1 N-peptide and C-terminal anchor in SNARE complex formation. Proc. Natl. Acad. Sci. U. S. A. *108*, 1040–1045.

Imig, C., Min, S.-W., Krinner, S., Arancillo, M., Rosenmund, C., Südhof, T.C., Rhee, J., Brose, N., and Cooper, B.H. (2014). The morphological and molecular nature of synaptic vesicle priming at presynaptic active zones. Neuron *84*, 416–431.

Jiao, J., He, M., Port, S.A., Baker, R.W., Xu, Y., Qu, H., Xiong, Y., Wang, Y., Jin, H., Eisemann, T.J., et al. (2018). Munc18-1 catalyzes neuronal SNARE assembly by templating SNARE association. ELife *7*.

Kaeser, P.S., Deng, L., Wang, Y., Dulubova, I., Liu, X., Rizo, J., and Südhof, T.C. (2011). RIM proteins tether Ca2+ channels to presynaptic active zones via a direct PDZ-domain interaction. Cell *144*, 282–295.

Kalyana Sundaram, R.V., Jin, H., Li, F., Shu, T., Coleman, J., Yang, J., Pincet, F., Zhang, Y., Rothman, J.E., and Krishnakumar, S.S. (2021). Munc13 binds and recruits SNAP25 to chaperone SNARE complex assembly. FEBS Lett. *595*, 297–309.

Lai, Y., Choi, U.B., Leitz, J., Rhee, H.J., Lee, C., Altas, B., Zhao, M., Pfuetzner, R.A., Wang, A.L., Brose, N., et al. (2017). Molecular Mechanisms of Synaptic Vesicle Priming by Munc13 and Munc18. Neuron *95*, 591-607.e10.

Larkin, M.A., Blackshields, G., Brown, N.P., Chenna, R., McGettigan, P.A., McWilliam, H., Valentin, F., Wallace, I.M., Wilm, A., Lopez, R., et al. (2007). Clustal W and Clustal X version 2.0. Bioinformatics *23*, 2947–2948.

Lee, S., Shin, J., Jung, Y., Son, H., Shin, J., Jeong, C., Kweon, D.-H., and Shin, Y.-K. (2020). Munc18-1 induces conformational changes of syntaxin-1 in multiple intermediates for SNARE assembly. Sci. Rep. *10*, 11623.

Lürick, A., Kuhlee, A., Bröcker, C., Kümmel, D., Raunser, S., and Ungermann, C. (2015). The Habc domain of the SNARE Vam3 interacts with the HOPS tethering complex to facilitate vacuole fusion. J. Biol. Chem. *290*, 5405–5413.

Ma, C., Li, W., Xu, Y., and Rizo, J. (2011). Munc13 mediates the transition from the closed syntaxin-Munc18 complex to the SNARE complex. Nat. Struct. Mol. Biol. *18*, 542–549.

Ma, L., Rebane, A.A., Yang, G., Xi, Z., Kang, Y., Gao, Y., and Zhang, Y. (2015). Munc18-1-regulated stage-wise SNARE assembly underlying synaptic exocytosis. ELife *4*, 1–30.

Magdziarek, M., Bolembach, A.A., Stepien, K.P., Quade, B., Liu, X., and Rizo, J. (2020). Re-examining how Munc13-1 facilitates opening of syntaxin-1. Protein Sci. Publ. Protein Soc. *29*, 1440–1458.

Mahoney, T.R., Luo, S., and Nonet, M.L. (2006). Analysis of synaptic transmission in *Caenorhabditis elegans* using an aldicarb-sensitivity assay. Nat. Protoc. *1*, 1772–1777.

McEwen, J.M., and Kaplan, J.M. (2008). UNC-18 promotes both the anterograde trafficking and synaptic function of syntaxin. Mol. Biol. Cell *19*, 3836–3846.

McEwen, J.M., Madison, J.M., Dybbs, M., and Kaplan, J.M. (2006). Antagonistic regulation of synaptic vesicle priming by Tomosyn and UNC-13. Neuron *51*, 303–315.

Medine, C.N., Rickman, C., Chamberlain, L.H., and Duncan, R.R. (2007). Munc18-1 prevents the formation of ectopic SNARE complexes in living cells. J. Cell Sci. *120*, 4407–4415.

Meijer, M., Burkhardt, P., De Wit, H., Toonen, R.F., Fasshauer, D., and Verhage, M. (2012). Munc18-1 mutations that strongly impair SNARE-complex binding support normal synaptic transmission. EMBO J. *31*, 2156–2168.

Merlini, L., Dudin, O., and Martin, S.G. (2013). Mate and fuse: how yeast cells do it. Open Biol. *3*, 130008.

Min, D., Kim, K., Hyeon, C., Cho, Y.H., Shin, Y.-K., and Yoon, T.-Y. (2013). Mechanical unzipping and rezipping of a single SNARE complex reveals hysteresis as a force-generating mechanism. Nat. Commun. *4*, 1705.

Misura, K.M.S., Scheller, R.H., and Weis, W.I. (2000). Three-dimensional structure of the neuronal-Sec1-syntaxin 1a complex. Nature *404*, 355–362.

Munch, A.S., Kedar, G.H., van Weering, J.R.T., Vazquez-Sanchez, S., He, E., André, T., Braun, T., Söllner, T.H., Verhage, M., and Sørensen, J.B. (2016). Extension of helix 12 in munc18-1 induces vesicle priming. J. Neurosci. *36*, 6881–6891.

Nicholson, K.L., Munson, M., Miller, R.B., Filip, T.J., Fairman, R., and Hughson, F.M. (1998). Regulation of SNARE complex assembly by an N-terminal domain of the t-SNARE Sso1p. Nat. Struct. Biol. *5*, 793–802.

Novick, P., and Schekman, R. (1979). Secretion and cell-surface growth are blocked in a temperature-sensitive mutant of *Saccharomyces cerevisiae*. Proc. Natl. Acad. Sci. U. S. A. *76*, 1858–1862.

Parisotto, D., Pfau, M., Scheutzow, A., Wild, K., Mayer, M.P., Malsam, J., Sinning, I., and Söllner, T.H. (2014). An extended helical conformation in domain 3a of Munc18-1 provides a template for SNARE (soluble N-Ethylmaleimidesensitive factor attachment protein receptor) complex assembly. J. Biol. Chem. *289*, 9639–9650.

Park, S., Bin, N.R., Rajah, M.M., Kim, B., Chou, T.C., Kang, S.Y.A., Sugita, K., Parsaud, L., Smith, M., Monnier, P.P., et al. (2016). Conformational states of syntaxin-1 govern the necessity of N-peptide binding in exocytosis of PC12 cells and *Caenorhabditis elegans*. Mol. Biol. Cell *27*, 669–685.

Park, S., Bin, N.R., Yu, B., Wong, R., Sitarska, E., Sugita, K., Ma, K., Xu, J., Tien, C.W., Algouneh, A., et al. (2017). UNC-18 and tomosyn antagonistically control synaptic vesicle priming downstream of UNC-13 in *Caenorhabditis elegans*. J. Neurosci. *37*, 8797–8815.

Pettersen, E.F., Goddard, T.D., Huang, C.C., Couch, G.S., Greenblatt, D.M., Meng, E.C., and Ferrin, T.E. (2004). UCSF Chimera--a visualization system for exploratory research and analysis. J. Comput. Chem. *25*, 1605–1612.

Pettersen, E.F., Goddard, T.D., Huang, C.C., Meng, E.C., Couch, G.S., Croll, T.I., Morris, J.H., and Ferrin, T.E. (2021). UCSF ChimeraX: Structure visualization for researchers, educators, and developers. Protein Sci. *30*, 70–82.

Pobbati, A. V, Stein, A., and Fasshauer, D. (2006). N- to C-terminal SNARE complex assembly promotes rapid membrane fusion. Science *313*, 673–676.

Rathore, S.S., Bend, E.G., Yu, H., Hammarlund, M., Jorgensen, E.M., and Shen, J. (2010). Syntaxin N-terminal peptide motif is an initiation factor for the assembly of the SNARE-Sec1/Munc18 membrane fusion complex. Proc. Natl. Acad. Sci. U. S. A. *107*, 22399–22406.

Richmond, J.E., and Jorgensen, E.M. (1999). One GABA and two acetylcholine receptors function at the *C. elegans* neuromuscular junction. Nat. Neurosci. *2*, 791–798.

Richmond, J.E., Davis, W.S., and Jorgensen, E.M. (1999). UNC-13 is required for synaptic vesicle fusion in *C. elegans*. Nat. Neurosci. *2*, 959–964.

Richmond, J.E., Weimer, R.M., and Jorgensen, E.M. (2001). An open form of syntaxin bypasses the requirement for UNC-13 in vesicle priming. Nature *412*, 338–341.

Rickman, C., Medine, C.N., Bergmann, A., and Duncan, R.R. (2007). Functionally and spatially distinct modes of munc18-syntaxin 1 interaction. J. Biol. Chem. *282*, 12097–12103.

Rodkey, T.L., Liu, S., Barry, M., and McNew, J.A. (2008). Munc18a scaffolds SNARE assembly to promote membrane fusion. Mol. Biol. Cell *19*, 5422–5434.

Rothman, J.E. (2014). The principle of membrane fusion in the cell (Nobel lecture). Angew. Chem. Int. Ed Engl. *53*, 12676–12694.

Rowe, J., Corradi, N., Malosio, M.L., Taverna, E., Halban, P., Meldolesi, J., and Rosa, P. (1999). Blockade of membrane transport and disassembly of the Golgi complex by expression of syntaxin 1A in neurosecretion-incompetent cells: Prevention by rbSEC1. J. Cell Sci. *112*, 1865–1877.

Rowe, J., Calegari, F., Taverna, E., Longhi, R., and Rosa, P. (2001). Syntaxin 1A is delivered to the apical and basolateral domains of epithelial cells: the role of munc-18 proteins. J. Cell Sci. *114*, 3323–3332.

Saifee, O., Wei, L., and Nonet, M.L. (1998). The *Caenorhabditis elegans unc-64* locus encodes a syntaxin that interacts genetically with synaptobrevin. Mol. Biol. Cell *9*, 1235–1252.

Schwede, T., Kopp, J., Guex, N., and Peitsch, M.C. (2003). SWISS-MODEL: an automated protein homology-modeling server. Nucleic Acids Res. *31*, 3381–3385.

Shen, J., Tareste, D.C., Paumet, F., Rothman, J.E., and Melia, T.J. (2007). Selective activation of cognate SNAREpins by Sec1/Munc18 proteins. Cell *128*, 183–195.

27

Shen, J., Rathore, S.S., Khandan, L., and Rothman, J.E. (2010). SNARE bundle and syntaxin N-peptide constitute a minimal complement for Munc18-1 activation of membrane fusion. J. Cell Biol. *190*, 55–63.

Shu, T., Jin, H., Rothman, J.E., and Zhang, Y. (2020). Munc13-1 MUN domain and Munc18-1 cooperatively chaperone SNARE assembly through a tetrameric complex. Proc. Natl. Acad. Sci. U. S. A. *117*, 1036–1041.

Sitarska, E., Xu, J., Park, S., Liu, X., Quade, B., Stepien, K., Sugita, K., Brautigam, C.A., Sugita, S., and Rizo, J. (2017). Autoinhibition of Munc18-1 modulates synaptobrevin binding and helps to enable Munc13-dependent regulation of membrane fusion. ELife *6*.

Smith, C.L., Varoqueaux, F., Kittelmann, M., Azzam, R.N., Cooper, B., Winters, C.A., Eitel, M., Fasshauer, D., and Reese, T.S. (2014). Novel cell types, neurosecretory cells, and body plan of the early-diverging metazoan *Trichoplax adhaerens*. Curr. Biol. *24*, 1565–1572.

Sørensen, J.B., Wiederhold, K., Müller, E.M., Milosevic, I., Nagy, G., de Groot, B.L., Grubmüller, H., and Fasshauer, D. (2006). Sequential N- to C-terminal SNARE complex assembly drives priming and fusion of secretory vesicles. EMBO J. *25*, 955–966.

Südhof, T.C. (2014). The molecular machinery of neurotransmitter release (Nobel lecture). Angew. Chem. Int. Ed Engl. *53*, 12696–12717.

Sutton, R.B., Fasshauer, D., Jahn, R., and Brunger, A.T. (1998). Crystal structure of a SNARE complex involved in synaptic exocytosis at 2.4 A resolution. Nature *395*, 347–353.

Tan, C., Wang, S.S.H., de Nola, G., and Kaeser, P.S. (2022). Rebuilding essential active zone functions within a synapse. Neuron S0896-6273(22)00083-6.

Taylor, S.R., Santpere, G., Weinreb, A., Barrett, A., Reilly, M.B., Xu, C., Varol, E., Oikonomou, P., Glenwinkel, L., McWhirter, R., et al. (2021). Molecular topography of an entire nervous system. Cell *184*, 4329-4347.e23.

Tien, C.-W., Yu, B., Huang, M., Stepien, K.P., Sugita, K., Xie, X., Han, L., Monnier, P.P., Zhen, M., Rizo, J., et al. (2020). Open syntaxin overcomes exocytosis defects of diverse mutants in *C. elegans*. Nat. Commun. *11*, 5516.

Toonen, R.F., Kochubey, O., de Wit, H., Gulyas-Kovacs, A., Konijnenburg, B., Sørensen, J.B., Klingauf, J., and Verhage, M. (2006). Dissecting docking and tethering of secretory vesicles at the target membrane. EMBO J. *25*, 3725–3737.

Vardar, G., Salazar-Lázaro, A., Brockmann, M., Weber-Boyvat, M., Zobel, S., Kumbol, V.W.-A., Trimbuch, T., and Rosenmund, C. (2021). Reexamination of N-terminal domains of syntaxin-1 in vesicle fusion from central murine synapses. ELife *10*.

Voets, T., Toonen, R.F., Brian, E.C., de Wit, H., Moser, T., Rettig, J., Südhof, T.C., Neher, E., and Verhage, M. (2001). Munc18-1 promotes large dense-core vesicle docking. Neuron *31*, 581–591.

Wang, S., Li, Y., Gong, J., Ye, S., Yang, X., Zhang, R., and Ma, C. (2019). Munc18 and Munc13 serve as a functional template to orchestrate neuronal SNARE complex assembly. Nat. Commun. *10*, 69.

Watanabe, S., Rost, B.R., Camacho-Pérez, M., Davis, M.W., Söhl-Kielczynski, B., Rosenmund, C., and Jorgensen, E.M. (2013). Ultrafast endocytosis at mouse hippocampal synapses. Nature *504*, 242–247.

Waterhouse, A.M., Procter, J.B., Martin, D.M.A., Clamp, M., and Barton, G.J. (2009). Jalview Version 2--a multiple sequence alignment editor and analysis workbench. Bioinforma. Oxf. Engl. *25*, 1189–1191.

Weimer, R.M., Richmond, J.E., Davis, W.S., Hadwiger, G., Nonet, M.L., and Jorgensen, E.M. (2003). Defects in synaptic vesicle docking in *unc-18* mutants. Nat. Neurosci. *6*, 1023–1030.

White, J.G., Southgate, E., Thomson, J.N., and Brenner, S. (1986). The structure of the nervous system of the nematode *Caenorhabditis elegans*. Philos. Trans. R. Soc. Lond. B. Biol. Sci. *314*, 1–340.

de Wit, H., Cornelisse, L.N., Toonen, R.F.G., and Verhage, M. (2006). Docking of secretory vesicles is syntaxin dependent. PloS One *1*, e126.

Xu, T., Rammner, B., Margittai, M., Artalejo, A.R., Neher, E., and Jahn, R. (1999). Inhibition of SNARE complex assembly differentially affects kinetic components of exocytosis. Cell *99*, 713–722.

Yang, X., Xu, P., Xiao, Y., Xiong, X., and Xu, T. (2006). Domain requirement for the membrane trafficking and targeting of syntaxin 1A. J. Biol. Chem. *281*, 15457–15463.

Yang, X., Wang, S., Sheng, Y., Zhang, M., Zou, W., Wu, L., Kang, L., Rizo, J., Zhang, R., Xu, T., et al. (2015). Syntaxin opening by the MUN domain underlies the function of Munc13 in synaptic-vesicle priming. Nat. Struct. Mol. Biol. *22*, 547–554.

Zhou, P., Pang, Z.P., Yang, X., Zhang, Y., Rosenmund, C., Bacaj, T., and Südhof, T.C. (2013). Syntaxin-1 N-peptide and Habc-domain perform distinct essential functions in synaptic vesicle fusion. EMBO J. *32*, 159–171.

Zorman, S., Rebane, A.A., Ma, L., Yang, G., Molski, M.A., Coleman, J., Pincet, F., Rothman, J.E., and Zhang, Y. (2014). Common intermediates and kinetics, but different energetics, in the assembly of SNARE proteins. ELife *3*, e03348.

A

worm Syntaxin

yeast chimeras

N-peptide   Habc   Linker   SNARE

1 mm

B   speed

yeast

n.s.

200

(μm/s)

100

0

***   ***   ***

(20)   (20)   (20)   (20)   (20)

worm Syx   N-peptide   Habc   Linker   SNARE
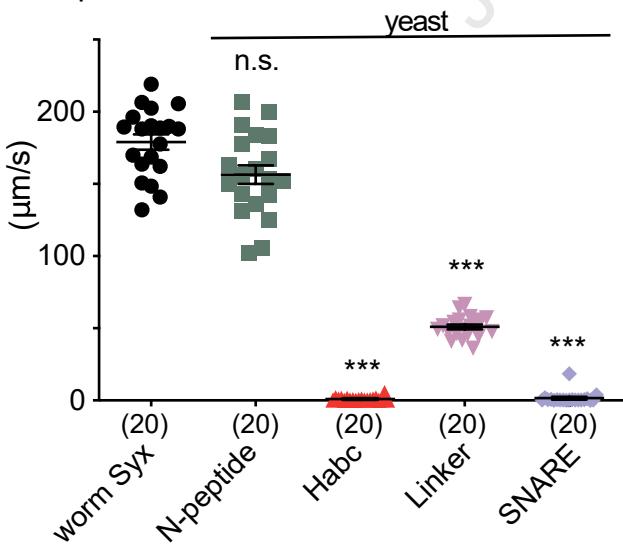
C   aldicarb sensitivity of yeast chimeras

100

Paralyzed animals (%)

50

0

0   100   200   300

time (min) in aldicarb

● worm Syx
■ N-peptide
▼ Linker
◆ SNARE
● Syx null
▲ Habc

A worm Syntaxin   Trichoplax Habc   Choanoflagellate Habc   yeast Habc

1mm

B speed

C aldicarb sensitivity

D mPSCs

E frequency mPSCs

A speed
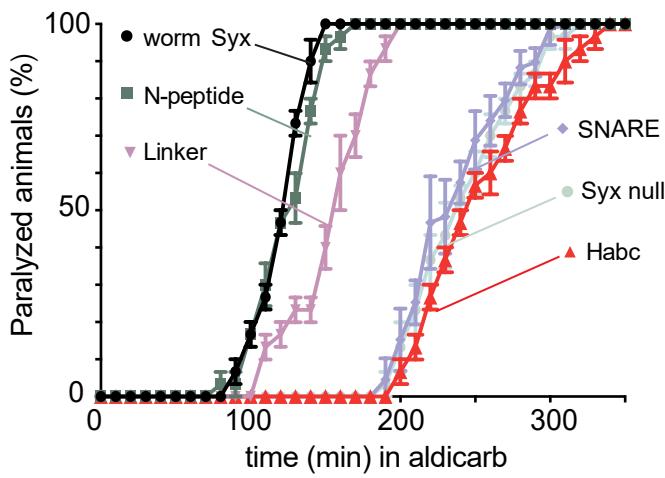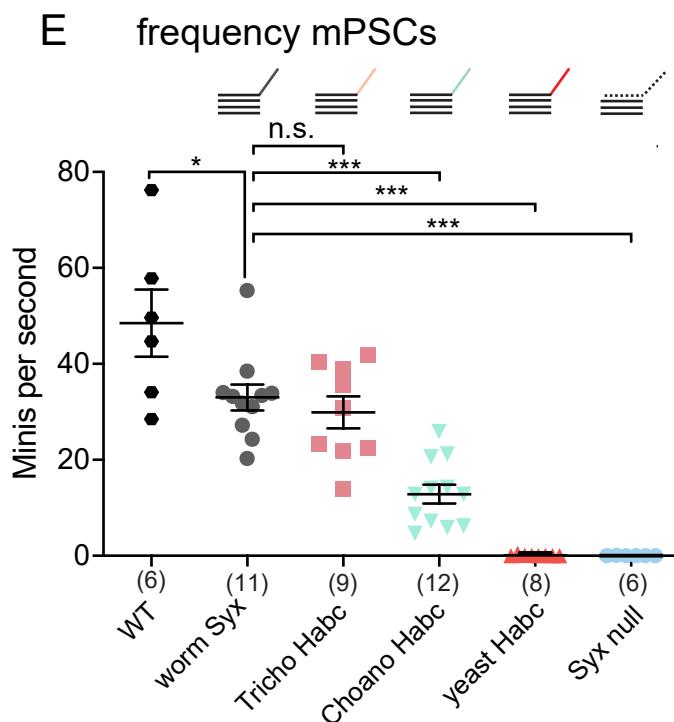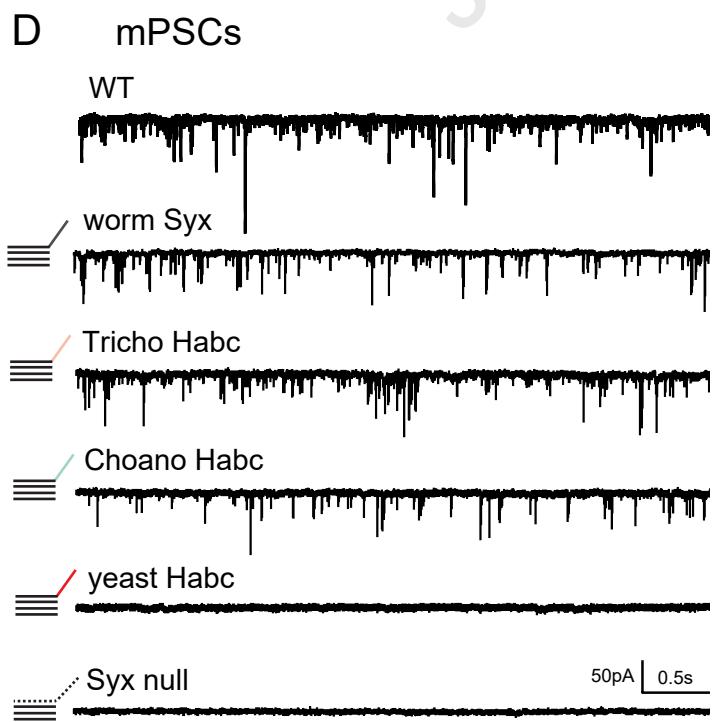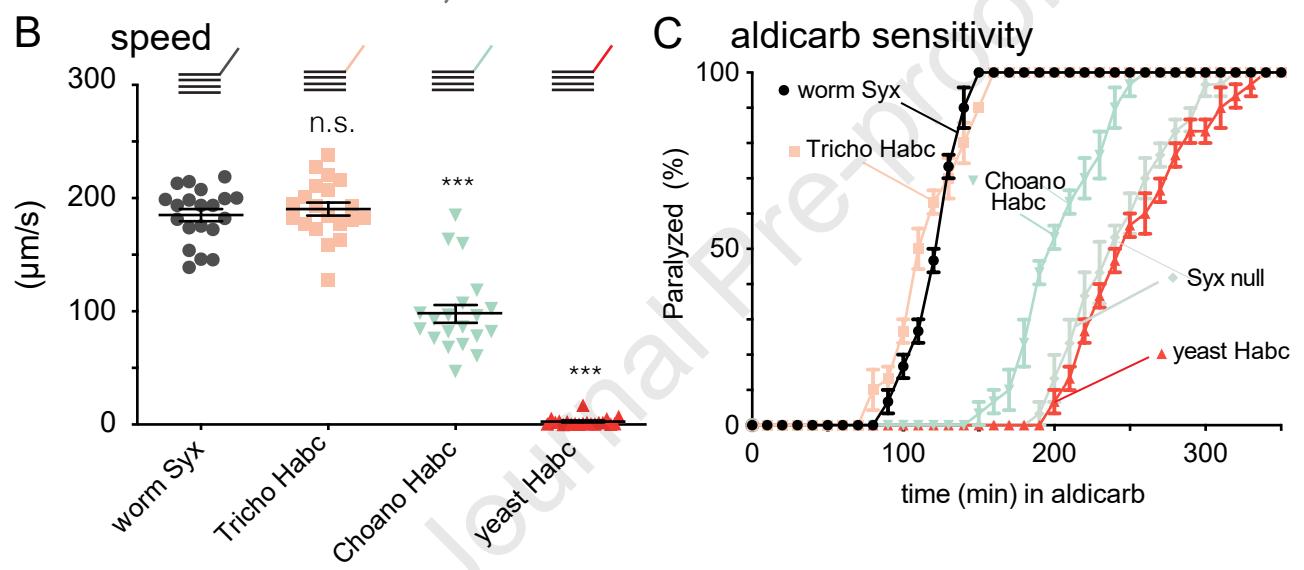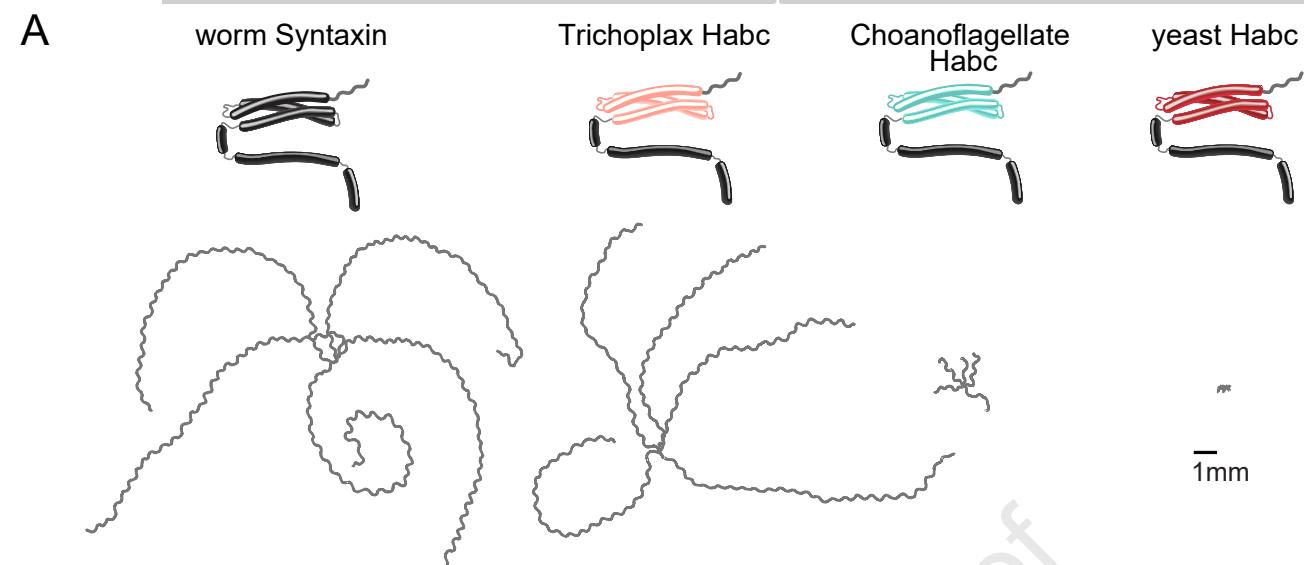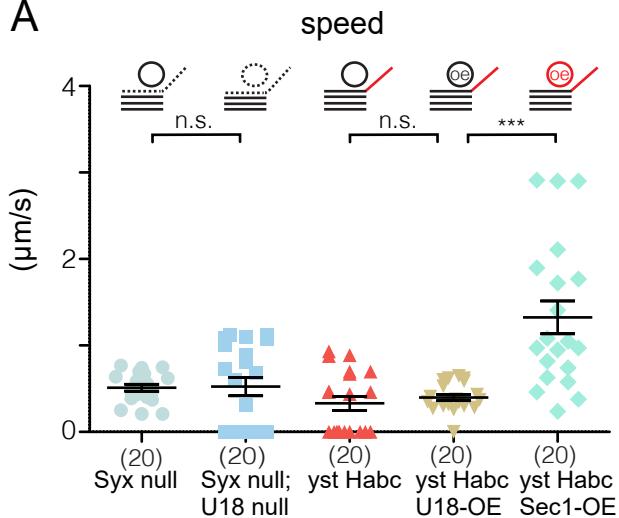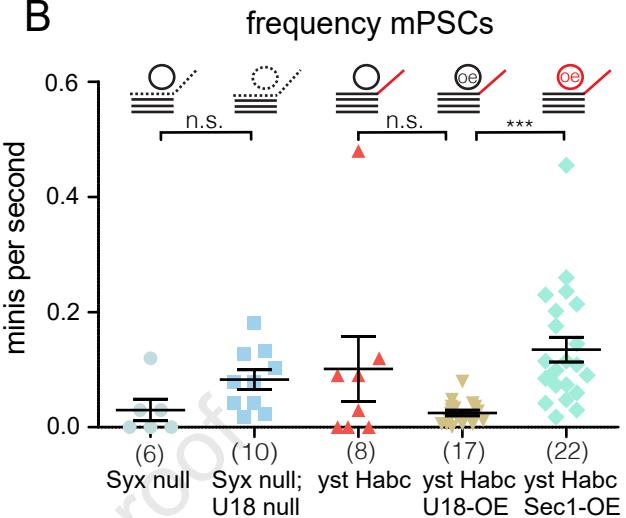
B frequency mPSCs

C mPSCs

D docking

E

A speed

B frequency mPSCs

C mPSCs

yeast Habc; OE Sec1

yeast Habc; OE yeast-worm Sec1

OE yeast SNARE complex; OE Sec1

OE yeast Habc-SNARE complex; OE Sec1

50pA

0.5s

D docking

n.s.

E

yeast Habc;
yeast-worm Sec1

yeast SNARE complex;
yeast Sec1

yeast Habc+SNAREs;
yeast Sec1

wild type

100 nm

A speed

B aldicarb sensitivity

C frequency mPSCs

D mPSCs

E

F docking

UNC-18

closed
syntaxin

UNC-18 chaperones
closed syntaxin

UNC-13

UNC-13 opens syntaxin

syntaxin Habc opens UNC-18

synaptobrevin

open UNC-18 templates
trans-SNAREs

complexin

SNAP-25
synaptotagmin C2B

nucleation of SNARE complex
fusion blocked by synaptotagmin
and complexin

"Interspecies complementation identifies a pathway to assemble SNAREs"

Highlights:

- Interspecies complementation identifies interactions between SM and SNARE proteins.
- Synaptic transmission requires UNC-18 to interact with SNARE and Habc domains.
- The Habc-SM interaction can be partially bypassed by an open form of UNC-18.
- Yeast SM and SNARE proteins can provide rescue of synaptic transmission.

KEY RESOURCES TABLE

REAGENT or RESOURCE	SOURCE	IDENTIFIER
Bacterial and Virus Strains		
Escherichia coli OP50	Caenorhabditis Genetics Center (CGC)	OP50
TOP10	Lab stock	N/A
Chemicals, Peptides, and Recombinant Proteins		
Aldicarb	ChemService	Cat# N-11044
Cyanoacrylate Glue	Aesculap Histoacryl; BBraun Inc.	https://www.bbraun.com/en/products/b/histoacryl.html
Collagenase	Sigma-Aldrich	Cat #C5138
Osmium tetroxide	EMS	Cat # 19110
Acetone, glass-distilled, electron microscopy grade	EMS	Cat # 10015
Glutaraldehyde	EMS	Cat # 111-30-8
Uranyl acetate	EMS	Cat # 22400
Sodium Azide	Thermo Fisher Scientific	Cat # 190385000
Critical Commercial Assays		
Gibson assembly	New England Biolabs	Cat # E2611S
Gateway cloning method	Invitrogen	N/A
Experimental Models: Organisms/Strains		
C. elegans: Bristol N2 (adult stage, hermaphrodite	Caenorhabditis Genetics Center (CGC)	N2
See Table S1 for all *C. elegans* strains used in this study	This paper	N/A
Recombinant DNA		
pBSK(+)Sec1p cDNA	Biomatik	https://www.biomatik.com/services/gene-synthesis.html
Software and Algorithms		
SWISS-MODEL Webserver	Schwede et al., 2003	https://swissmodel.expasy.org
Clustal Omega	Higgins and Sharp, 1988	http://www.clustal.org/omega
ImageJ	Schneider et al., 2012	https://imagej.nih.gov/ij/
WormLab		https://www.mbfbioscience.com/wormlab
Prism	GraphPad	Version 8.3
ApE	Davis and Jorgensen, 2022	https://jorgensen.biology.utah.edu/wayned/ape/
Patchmaster	HEKA Elektronik	https://www.heka.com

IGOR Pro	WaveMetrics	IGOR Pro 8
MiniAnalysis	Synaptosoft	N/A
Jalview	Waterhouse et al., 2009	https://www.jalview.org/
Chimera and Chimera X	Pettersen et al., 2004, 2021	https://www.cgl.ucsf.edu/chimerax/